The Effect of Novel Longitudinal Branched Fins on the Performance of the Latent Heat Accumulator based on Shell-and-Tube Configuration

Ahmed E. Amer *‡, Vladimir A. Lebedev **,

Mohamed M. Elsakka ***

* Mechanical Power Engineering Department, Faculty of Engineering, Port Said University, Egypt

** Heat Engineering and Heat Power Engineering Department, Faculty of Energy, Saint-Petersburg Mining University, Russia

*** Mechanical Power Engineering Department, Faculty of Engineering, Port Said University, Egypt

(eng.ahmed_amer@eng.psu.edu.eg, lebedev_va@spmi.ru, elsakka@eng.psu.edu.eg)

‡ Corresponding Author; Ahmed E Amer, 42526, Port Said, Egypt, Tel: + 020 66 340 3459,
Fax: +020 66 340 0936, eng.ahmed_amer@eng.psu.edu.eg

Received: 12.01.2023 Accepted:03.03.2023

Abstract- A latent heat accumulator unit in the shape of a horizontal Shell-and-Tube (S-T) configuration with novel patented branched Fins was numerically studied. First, the numerical results have been validated with available experimental data of a horizontal S-T accumulator unit without fins. The results show agreement with experimental data. The numerical results are based on a 2D simulation performed using ANSYS FLUENT software. The horizontal S-T accumulator unit is investigated in two physical designs: (1) horizontal S-T accumulator with 6 longitudinal fins, and (2) horizontal S-T accumulator with novel longitudinal branching fins. The paraffin wax is utilized as the phase change material (PCM). The selected PCM is used to fill the annular space of the proposed accumulator unit. The temperature of the inner tube wall is kept constant to represent the heat transfer fluid (HTF) temperature. Also, this temperature was set to 358 K (85 °C) during charging and 301 K (28 °C) during the discharging. The thermal performance of the charging and discharging processes for two-physical designs was explained. The numerical results show that the PCM takes about 110 minutes to be completely melted and 250 minutes to be completely solidified for a horizontal S-T accumulator with 6 longitudinal fins. For horizontal S-T accumulator with novel longitudinal branching fins, the PCM takes about 55 minutes to be completely melted and 80 minutes to be completely solidified. The numerical results indicated that using novel branched longitudinal fins enhances heat transfer. Furthermore, it is observed that the novel fins lead to a significant reduction in the solidification and the melting times by about 68 % and 50 % respectively, in contrast with the ordinary longitudinal fins. The novelty of this paper is the investigation of new patented branched fins for a PCM accumulator in both the melting and solidification scenarios. In contrast with the traditional longitudinal fins, it is observed from the numerical results that the utilization of the novel patented branched fins always improves the performance of the accumulator.

Keywords Accumulator; Thermal energy storage; Longitudinal Branched Fins; Melting time rate; Numerical study.

1. Introduction

There is increasing research in improving renewable energy systems [1]-[12]. Researchers resort to developing different techniques for storing energy in times of partial load and times of its availability to improve its use later in times of need, as some energy sources are less and others are not available all the time, such as solar energy. Furthermore, there are several forms to store energy, including chemical, thermal, electrical, and mechanical energy. Various techniques are used to store thermal energy. Moreover, the thermal energy could be stored in two forms, either latent heat or sensible heat. This is done through materials for storing thermal energy and divided into storage materials for sensible energy and materials for storing latent energy called phase-changing materials. There are many of these materials that are currently employed in several practical applications like space, buildings, and several solar energy systems.[13]–[18]. There are criteria for selecting these materials, including that the melting temperature is compatible with the required application and has large potential energy and other known criteria. Mathematical methods can be used to choose the appropriate materials for the application using the Analytic hierarchy process (AHP) procedure [19]–[21]. Some applications require storage for large times and others for short times. Most materials do not meet all standards and have low thermal conductivity. Therefore, researchers resort to using methods to increase heat transfer, such as fins, nanomaterials, and other methods. Many researchers used the shell and tube configuration for storing the thermal energy using the phase change materials (PCM) [22]–[26]. Jawad et al. [27] investigated the influence of adding paraffin wax with the aluminium chip, and nano-SiC in improving the performance of solar air heaters. Their findings indicated that the implementation of the PCM with the aluminium chip, and nano-SiC allowed for increasing the working time by at least 3h after the sunset. Sulaiman et al. [28] found that an increase of up to 60% in the photovoltaics thermal efficiency can be achieved by implementing paraffin wax. Many researchers investigated several types of fin configurations such as annular and longitudinal. Chaichan et al. [29] demonstrated that the use of hybrid paraffin (50% wax + 50% Vaseline) has a good potential in improving the productivity of Photovoltaic thermal systems. Amer et al. [30] studied the effects of implementing circumferential or circular-type fins around the inner cylinder of a fluid flow. The results have proven that there has been an enhancement in the heat transfer associated with the addition of the fins until it reached the optimum value, after which there was no change, as the size of the fins was fixed. Tay et al. [31] studied and validated three different models of thermal storage systems. It has been noticed that the implementation of fins is more favorable in heat transfer than using pinned surface. Ravi et al. [32] investigated the behavior of heat transfer in a circular tube configuration with PCM. They utilized internal longitudinal fins. It has been concluded that the height of the fins, the thermal conductivity of fins, and Stefan number have a great influence on the Nusselt number. Ismael et al. [33] presented a numerical model around a vertical tube with axially aligned fins that is immersed in the PCM during the solidification process. The numerical results indicated that increasing the length, thickness, and number of fins would lead to a significant reduction in the solidified mass fraction as well as solidification time. Deng et al. [34] proposed latent heat thermal-energy storage (LHTES). The proposed unit utilizes a new fin shape that aims at improving the heat transfer. Their results demonstrated that the value of thermal conductivity of shell material has substantial influence on the performance of fins heat transfer as well as the PCM melting behaviors. The required complete melting time of the PCM decreases when heat-transfer fluid temperature increases. The proposed performance of LHTES based on local double-fin would be significantly enhanced by employing longer fins. Aly et al. [35] numerically investigated the utilization of the longitudinal corrugated fins that are installed to increment the PCM solidification rate. Based on the simulation results, the solidification time has been reduced by implementing the novel corrugated fins in contrast with the straight fins. However, the straight fins are generally found to have higher effectiveness. There is a shortage of research that aims to improve the performance of the bottom of the horizontal S-T accumulator unit while this part takes more time for melting and solidification. So that this research presented a novel patent accumulator unit using branched fins [36]. The novelty of this paper is the investigation of new patented branched fins for a PCM accumulator in both the melting and solidification scenarios. The objective of this paper is to investigate the effect of the novel patented branched fines on the improvement of PCM accumulator performance.

2. Numerical Methods

2.1. *Numerical model and procedure*

The current simulations are carried out based on Computational Fluid Dynamics (CFD). Furthermore, ANSYS FLUENT software has been utilized in 2D mode using Reynolds-averaged Navier-Stokes equations, which is also referred to as RANS equations. An S-T latent heat accumulator unit is considered in a horizontal arrangement. Due to the relatively high flow rate, there are not many differences in the temperatures along the axial direction. Therefore, only the cross-section plane of the accumulator is considered in a 2D domain to reduce computational time. To consider effects of heat transfer, the energy equation is employed. The Boussinesq approximation was implemented to define the fluid density. This approximation varies the fluid density in the body force term while keeping it as a invariant value for all the governing equations. Moreover, the enthalpy-porosity formulation [37] is employed. This formulation is implemented for modelling of the melting process. The solidification and melting models are modeled with the aid of the enthalpy-porosity method along with finite-volume approach [38]. Also, the viscous dissipation and the change in volume of PCM throughout the melting process have been ignored. The detailed properties of the considered PCM material are available in [30]. The pressure staggering option (PRESTO) scheme has been implemented in transient simulation for spatial discretization of pressure. This is selected to provide more precise results by avoiding the interpolation errors in the standard discretization algorithm. The pressure-velocity coupling was based on the coupled solver method. The second-order upwind scheme has been implemented in order to account for the spatial discretization of both the energy and momentum equations. The selected numerical grid sizes are 9000 and 13000 for the longitudinal fins and branched fins. The selected mesh resolution is based on a recent mesh independency study [30]. A time-step size of about 0.1 s has been implemented based on a recent recommendation by Amer et al. [30].

In order to validate the numerical predictions, the numerical results are emphasized against the available experimental data provided by Hosseini et al. [39]. The experimental data of the horizontal S-T accumulator unit are used for comparison with numerical results for validation as shown in Fig. 1. Consequently, it is noticed that the numerical prediction of the model shows a good agreement in comparison with the available experimental data.

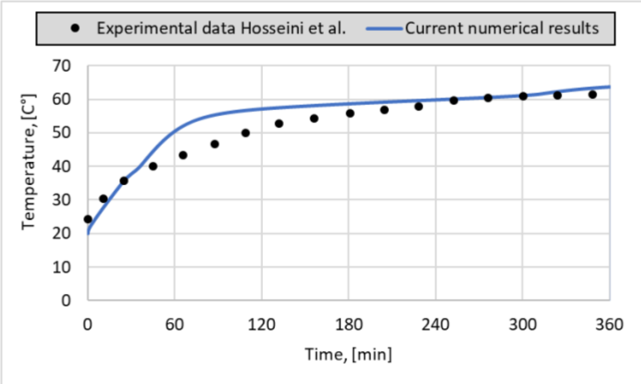

Fig. 1 A comparison between the experimental data presented by Hosseini et al. [39] for horizontal S-T accumulator and the corresponding numerical predictions.

2.2. *The physical model with traditional and novel longitudinal branched fins*

The two-physical designs of the horizontal latent heat accumulator unit are considered. The first is the S-T accumulator with 6 longitudinal fins while the second is the S-T accumulator with the novel longitudinal branched fins. Fig. 2 shows a schematic diagram that represents the horizontal S-T accumulator with 6 longitudinal fins. The accumulator unit consists of two concentric tubes. The central tube has an outer and inner diameter of 35 mm and 33 mm. In addition, the shell has an inner diameter of 128 mm. Axial copper fins are employed on the outer surface of the inner tube. Each fin has a thickness of 0.5 mm and a height of 44 mm. The fins are equally distributed with an angle of 60°. Paraffin wax is used as a PCM to store the thermal energy and is used to fill the annular space. In the outer tube, the external surface is well-insulated. Fig. 3 shows a schematic diagram of novel longitudinal branched fins. It consists of 6 longitudinal fins with the same dimensions as the previous diagram. Each fin includes 4 primary branched fins with a height of 20mm and 0.5mm thickness and 8 secondary branched fins with a height of 10mm and 0.5mm thickness

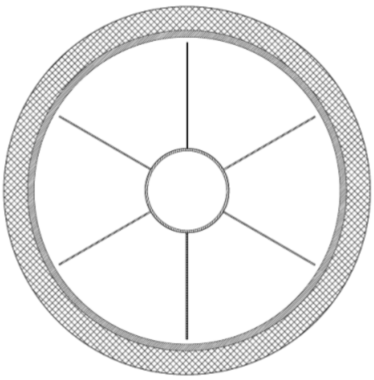

Fig. 2 The horizontal S-T with 6 longitudinal fins.

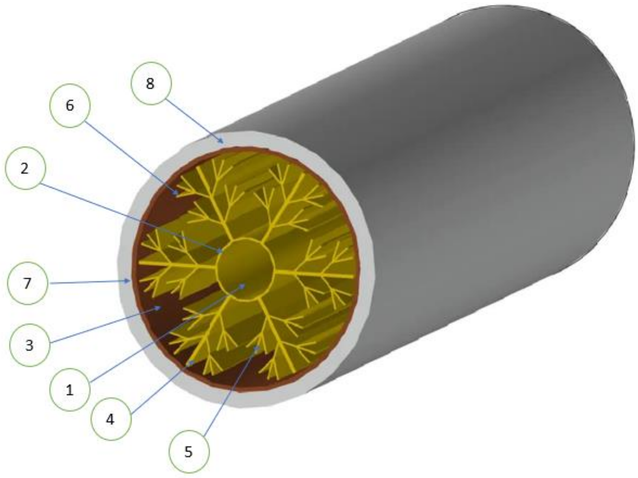

1. Heat Transfer Fluid
2. Inner pipe (tube)
3. Heat storage material
4. Fins
5. Branches of the 1st order
6. Branches of the 2nd order
7. Shell (cylinder)
8. Thermal insulation.

Fig. 3 A schematic diagram of novel longitudinal branched fins.

2.3. *Initial and boundary conditions*

The initial temperature of the utilized PCM, during the melting simulations, is set to 30 °C (303 K). However, the initial temperature is set to be 80 °C (353 K) during the solidification process. In addition, the HTF temperature is set to 85 °C (358 K) throughout the charging process while being 28 °C (301 K) in the case of discharging. The HTF temperature is represented by a constant temperature of the inner tube wall as recommended in [40]–[41]. The outer surface is associated with a wall boundary condition with zero heat flux.

3. Results and discussion

3.1. *Longitudinal Fins during Charging Process*

The contours of the predicted melt fraction and temperatures for the PCM in the accumulator unit for various times are shown in Fig. 4 and Fig. 5 for the longitudinal fins configuration. At starting, the heat from the inner hot tube is transferred to the solidified PCM by means of conduction before the PCM starts melting. This means that conduction dominated the melting process throughout the early stage. Accordingly, a relatively small portion of the melt paraffin has been formed around the surface of longitudinal fin as well as the hot wall of the inner tube of the accumulator. This melted portion is formed mainly by means of the conduction heat transfer mechanism only. The average liquid fraction is found to be about 24.3 % after 10 minutes. In the vicinity of fins, the solid paraffin is melted initially with a higher melting rate in contrast with the melting rate of the paraffin far from the fins. Owing to the influence of the natural convection, the region of melted paraffin around the upper fins is larger than the bottom fins.

As the time elapses, more liquid films of molten paraffin adjacent to the fin surface is formed during phase transition, thus providing a growing space for local natural convection. Then, heat transfer based on the buoyancy-induced natural convection is considered as the predominant mechanism in the melted PCM due to temperature differences. As evident, the molten paraffin in the upper part has a higher melting rate in contrast with the bottom part. This is owing to the local improvement in the transfer of melting heat. For the first 50 minutes of the melting process, it can be observed that the value of average liquid fraction is rapidly increased to about 86.8 %. The reasons are the high temperature of the liquid PCM along with the predominant influence of natural convection. After the rapid increase, there is a reduction in the rate of increasing liquid fraction. This reduction is occurring as the difference between the PCM and inner tube temperatures decreases. The decrease in the temperature differences is associated with a lower rate of heat transfer. Additionally, the increase in the thickness of the low conductivity melt PCM leads to an increment in the value of thermal resistance that consequently affects the heat transfer in the region between the surface of the hot inner tube and the solid-liquid phase interface. The rest solid part of paraffin 13.2 % took about 60 min to be completely melted. The PCM (paraffin wax) took almost 110 minutes (1.83 hours) to be completely melted.

3.2. *The Longitudinal Fins during Discharging Process*

The contours of the predicted solidification fraction and temperatures for the PCM in the accumulator unit for various times are shown in Fig. 6 and Fig. 7. At the beginning of discharging, the heat is transferred to the adjacent inner cold wall of the tube from the nearby liquid PCM by the conduction mechanism. The conduction mechanism is found to be predominant during the solidification process due to the rapid decline in the PCM temperature. This is owing to the relatively rapid reduction in the PCM temperature that reaches the PCM solidified temperature. As a result, in the vicinity of the longitudinal fins and the relatively cold wall of the inner tube, a small portion of solidified paraffin is formed by conduction. It can be therefore observed that the average solidified fraction is about 19.05 % after 10 minutes. Initially, the solidification rate of the liquid paraffin near the fins is higher in contrast with the solidification rate far from the fines. The solidified paraffin around the bottom fins is larger than the upper fins owing to the reduction in the natural convection. The natural convection assists in the upward movement inside the liquid PCM in addition to the downward motion of the solidified PCM in the beginning solidification process until 10 minutes.

With time elapsed, more solidified paraffin is formed during phase transition. In the first 50 minutes during solidification, the solidified fraction is found to increase with time to about 54.3 %. As the solidified fraction increases, the temperature of the solidified part of paraffin is reduced to wall temperature. As the time elapses, the rate of increase in the solid fraction is apparently reduced due to the temperature difference between the inner tube cold wall the and the adjacent PCM is reduced. The reduction in temperature differences leads to a reduction in heat transfer. After 100 minutes, the average solidified fraction reaches about 75.2 %. The rest part of the paraffin, i.e., 24.8 %, took about 150 min to be completely solidified. The PCM (paraffin wax) takes about 250 minutes (4.16 hours) to be completely solidified.

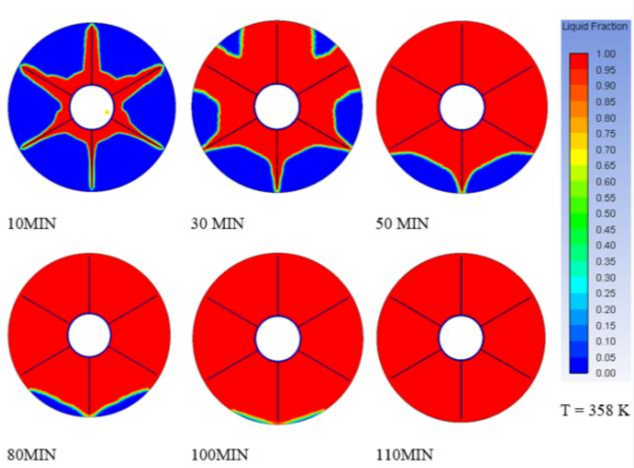

Fig. 4 Melt fraction contour of longitudinal fins.

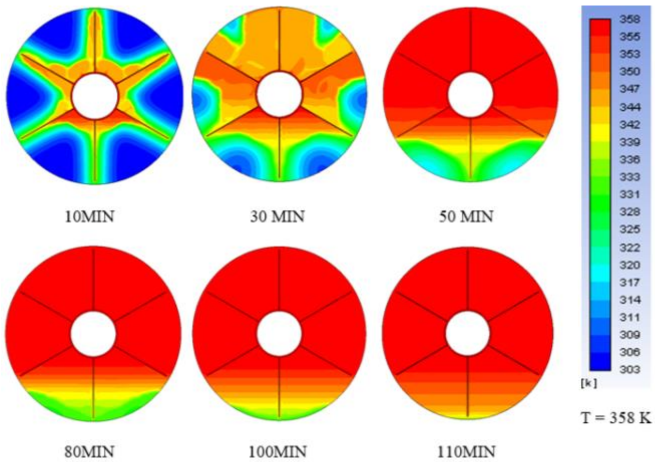

Fig. 5 Temperatures contour of longitudinal fins during melting during the melting process.

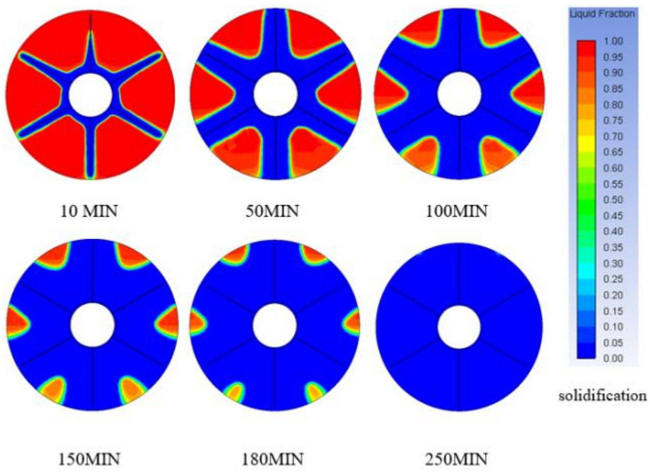

Fig. 6 Melt fraction contour of longitudinal fins during the solidification process.

3.3. The novel branched longitudinal fins during the Charging Process

The contours of temperature and melt fraction of PCM in the considered accumulator unit that employs the novel branched fins are shown in Fig. 8 and Fig 9 at different times. At starting, the heat is transferred by conduction between the hot surface of the inner tube and the adjacent solid PCM before the melting process of PCM starts. The conduction heat transfer mechanism is found to predominate the melting process during its early stage. Consequently, a relatively small portion of melt paraffin is formed in the region around the branched longitudinal fins as well as the hot wall of the tube. Moreover, the temperature in the molten region is increased as the energy is absorbed as sensible heat. The average liquid fraction is found to be about 29.6 % after 10 minutes. The rate of melting is higher in the adjacent regions around the proposed branched fins in contrast with the rate of melting far from the fins. The melted paraffin around the upper branched fins is greater than the bottom fins owing to the natural convection effects.

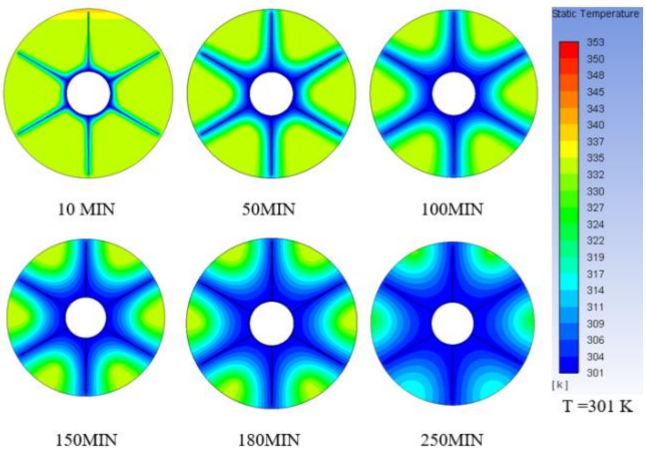

Fig. 7 Temperatures contour of longitudinal fins during the solidification process.

As the time elapses, more molten PCM adjacent to the fin surface is formed during phase transition, thus providing a growing space for local natural convection and then the buoyancy-induced natural convection is observed to predominate the heat transfer process in the melted PCM due to the temperature differences. It is observed that, in the upper part, the molten PCM has a higher melting rate than in the bottom part. The reason is that each of the conduction and the convection heat transfer is enhanced. As the time elapses, it is found that the liquid fraction increases in all directions across the accumulator tube.

In the first 40 minutes, the average value of the liquid fraction is rapidly increased to a value of 96.3 %. Then, there is a considerable reduction in the rate of change of the liquid fraction and this is associated with the lower temperature differences between hot inner tube wall and adjacent PCM. The reduction in temperature differences leads to a reduced rate of heat transfer. Furthermore, the increase in the thickness of the melt PCM leads to an increase in the thermal resistance. This significantly affects the rate of heat transfer in the region between the solid-liquid phase interface and the surface of hot inner tube. Using the branched fins, the total time required for reaching a complete melting state is about 55 minutes.

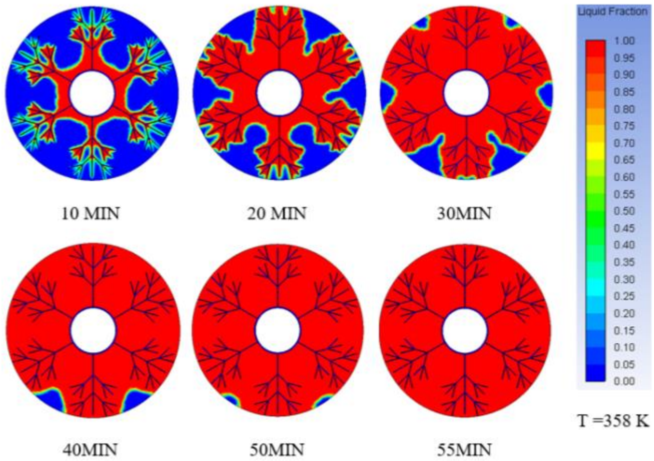

Fig 8 Melt fraction contour of longitudinal fins with branches fins during melting process.

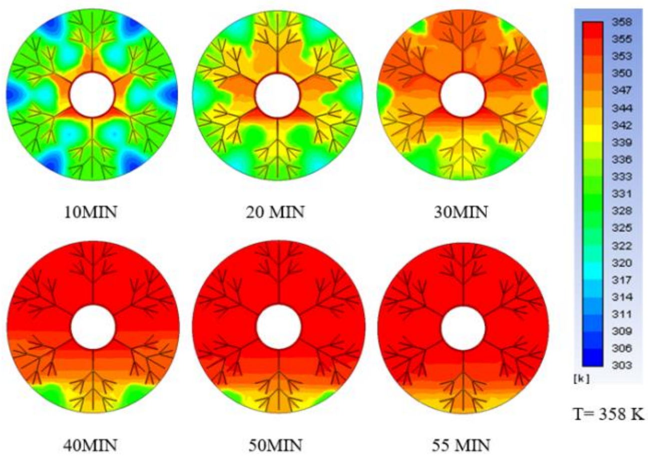

Fig. 9 Temperatures contour of longitudinal fins with branches fins during the melting process.

3.4. Discharging Process for Novel Branched Longitudinal Fins

The contours of the temperature and the solidified fraction in the proposed unit with the novel branched fins are shown in Fig. 10 and Fig. 11 at different times. At starting discharging, a region of solidified PCM has been formed in the area around the adjacent cold wall of fins and inner tube. The heat transfer occurs between the PCM and the HTF by thermal conduction mechanism. The reason is the considerable fast reduction in the PCM temperature that reaches solidification temperature of PCM. As a result, a large portion of solidified paraffin is formed in the region around the surface of the branched longitudinal fins and the cold tube wall due to the heat transfer taking place by means of conduction. Therefore, it is observed that the average solidified fraction was about 54.4 % after 10 minutes. At the beginning of the solidification process, it is found that the liquid PCM adjacent to the fin surfaces is solidified with a higher rate of solidification in contrast with the rate of solidification far from the fin surfaces. It is concluded that the branched longitudinal fins enhanced heat transfer rate and hence increased the rate of solidification.

With time elapsed, a larger region of solidified paraffin is developed through phase transition. After 30 minutes, the average solidified fraction reaches about 96.5 %. Then, it is observed that, the rate at which the solidified fraction increases, is reduced. The reason is that the differences in temperature between the cold inner tube wall and the PCM are reduced. This reduction in the differences of temperature leads to reducing the rate of heat transfer becomes slowly. In addition, the thick solidified layer increases the thermal resistance within the PCM. However, the rest part of the paraffin 3.5 % took about 50 min to be completely solidified. The PCM (paraffin wax) takes about 80 minutes (1.33 hours) to be completely solidified.

3.5. *Comparison between longitudinal fins and novel branched longitudinal fins during the melting process*

The comparison between the contours of melt fraction and temperature the PCM in accumulator unit with longitudinal fins as well as novel branched longitudinal fins are illustrated in Fig. 12, Fig. 13, and Fig. 14 at different times throughout the melting process. The average liquid fraction is observed to be about 24.3 % and 29.6 % after 10 minutes for longitudinal fins and novel branched longitudinal fins, respectively. It is concluded that the branched fins have a good potential in increasing the average liquid fraction in the first 10 minutes. In the temperature contours, the temperatures of paraffin for novel branched longitudinal is higher than longitudinal fins. After 20 minutes, the effect of branched fins becomes high where the average liquid fraction reaches 66.3 % while the average liquid fraction of longitudinal fins reaches 45.9 %. After 40 minutes, the upper part of paraffin is completely melted in novel branched longitudinal fins and the small part rest of the solid paraffin remains at the bottom between the regions of branched longitudinal fins. In the longitudinal fins, the small part rest of solid paraffin remains in the middle close to the outer tube and the bigger part remains in the bottom. About 55 minutes is required for the Paraffin wax to be completely melted in novel branched longitudinal fins while it takes about 110 min in traditional longitudinal fins. The numerical predictions indicated that the utilization of the novel branched longitudinal fins enhances the heat transfer and hence can assist in reducing the melting time by about 50 % compared to longitudinal fins. This is a much greater improvement in contrast with the previous results in the literature [14]-[26].

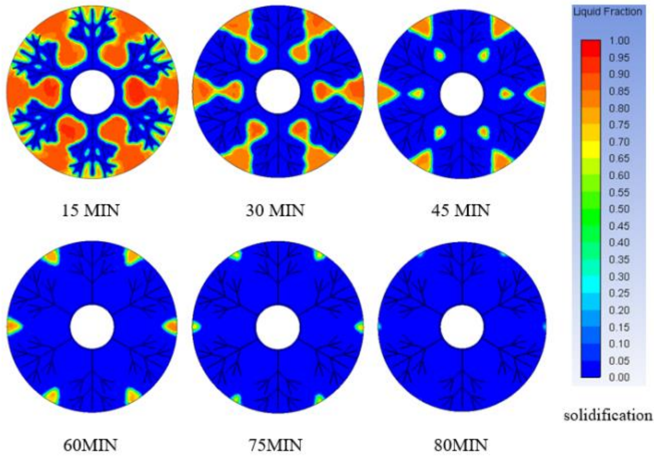

Fig 10 Melt fraction contour of longitudinal fins with branches fins during the solidification process.

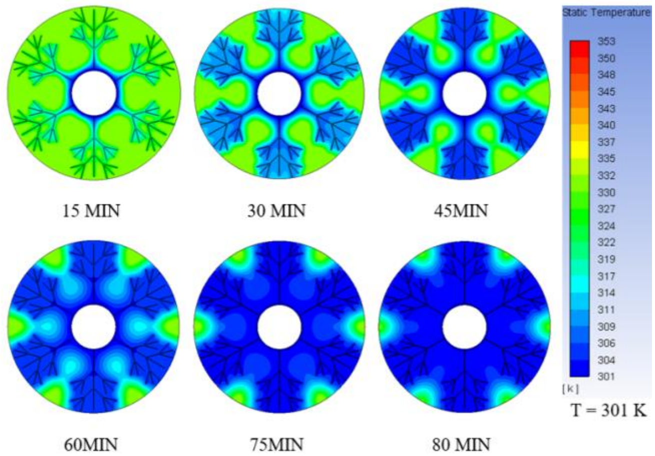

Fig 11 Temperatures contour of longitudinal fins with branches fins during the solidification process.

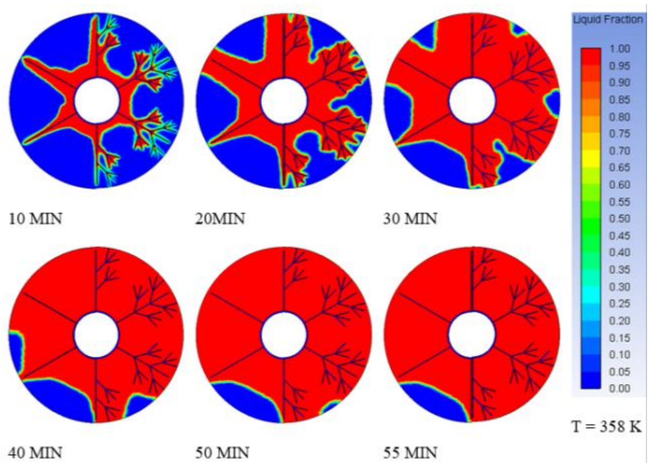

Fig. 12 Melt fraction contour of longitudinal fins and longitudinal fins with branches fins during the melting process.

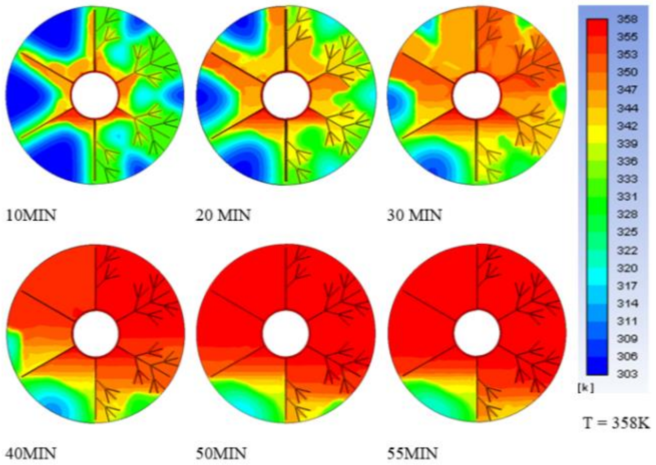

Fig. 13 Temperatures contour of longitudinal fins and longitudinal fins with branches fins during the melting process.

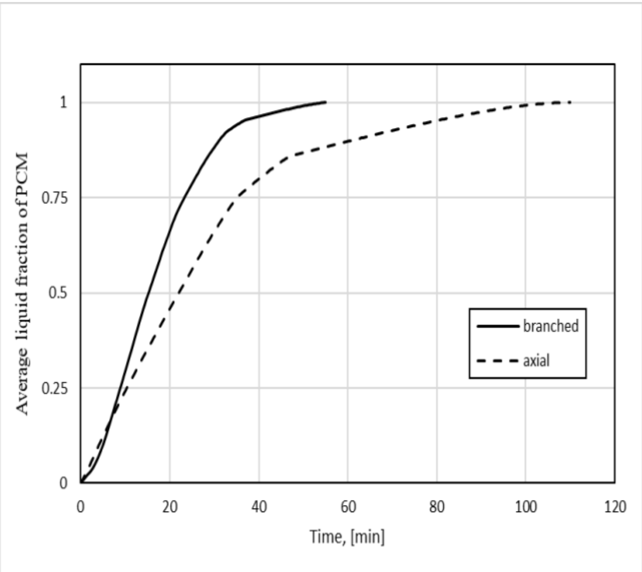

Fig. 14 The effect of two configurations of fin on the formation of the liquid fraction of the paraffin wax during the melting process.

3.6. *Comparison between longitudinal fins and novel branched longitudinal fins throughout the solidification process*

A comparison between the solidified fraction and the temperature contours of the PCM in the accumulator unit considering the longitudinal fins and novel branched fins during solidification process is depicted in Fig. 15 and Fig. 16 at different times. Furthermore, Fig. 17 shows a comparison between the average solidified fraction over time for the longitudinal fins and novel branched fins.

A rapid reduction in temperatures of paraffin due to loss of sensible heat in both of configurations is observed. It is noted that the average solidified fraction was about 19.05 % and 39.6 % after 10 minutes for longitudinal fins and novel branched longitudinal fins. The implementation of branched fins results in an increment of the rate of heat transfer by conduction and hence remarkably increase the solidified fraction in the first 10 minutes. In the temperature contours, the temperatures of paraffin for novel branched longitudinal is lower than longitudinal fins. After 30 minutes, the solidified fraction reaches to 79.03 % while the solidified fraction of longitudinal fins reaches 41.14 %.

After 50 minutes, the largest part of paraffin is solidified in novel branched longitudinal fins where the solidified fraction reaches to 93.3 % and small part rest of the paraffin remains between the regions of branched longitudinal fins. In the longitudinal fins, a large part of paraffin remains unsolidified in the region between the fins where the solidified fraction reaches 54.3 %. Paraffin wax takes about 80 minutes to be completely solidified in novel branched longitudinal fins while it takes about 250 min in longitudinal fins. In addition, the results referred that the use of the novel branched longitudinal fins is enhancing the predicted heat transfer rate and hence reducing the solidification time of the PCM by almost 68 % compared to longitudinal fins.

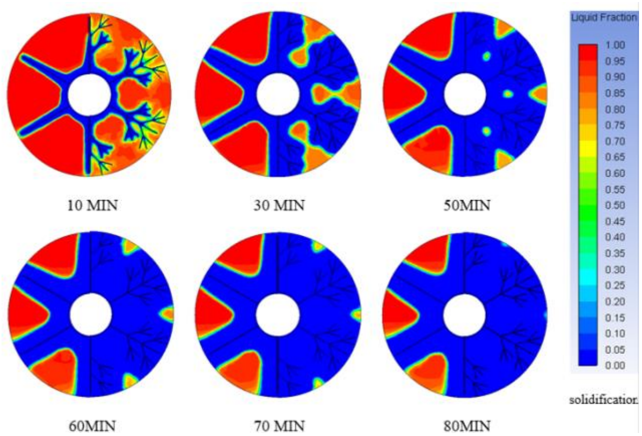

Fig. 15 Melt fraction contour of longitudinal fins and longitudinal fins with branches fins during the solidification process.

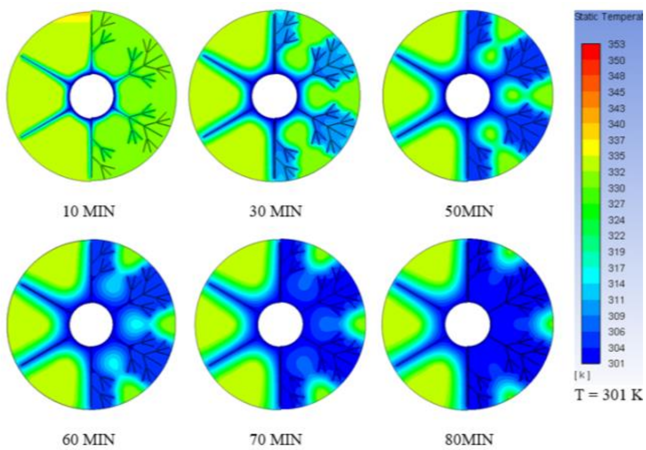

Fig. 16 Temperatures contour of longitudinal fins and longitudinal fins with branches fins during the solidification process.

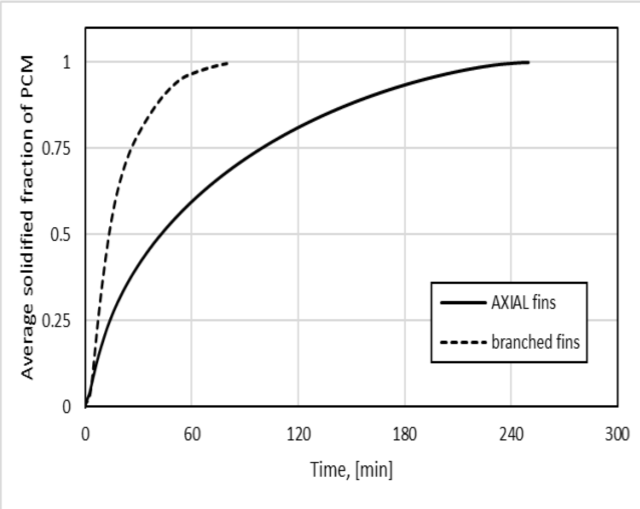

Fig. 17 The effect of two configurations of fin on the formation of the solidified fraction of paraffin wax during the discharging process.

4. Conclusion

The thermal performance of PCM throughout both the melting and solidification processes within a horizontal S-T accumulator employing a novel branched fins is numerically studied. Two physical designs of the horizontal S-T accumulator unit are investigated: (1) horizontal S-T accumulator with 6 longitudinal fins, and (2) horizontal S-T accumulator with new longitudinal branching fins. Simulations have been performed to investigate the influence of the suggested branched fins on both the complete melting and the solidification time inside the horizontal S-T accumulator unit. The transient behavior of the melting and solidification of the PCM in the two physical designs was investigated. Numerical results obtained in this study were validated against the available published experimental results. The comparison between the two-physical designs of the latent heat accumulator unit was numerically studied during the melting as well as the solidification process. Furthermore, the numerical results indicated that, by utilizing the novel branched longitudinal fins, the heat transfer process by means of conduction combined with natural convection are enhanced. Therefore, the melting time and the solidification time are found to be reduced by almost 50 % and 68 %, respectively compared to longitudinal fins. Based on the demonstrated improvements in the accumulator performance, the experimental investigation of the accumulator with the proposed branched fins is recommended for future works.

Acknowledgments

Ahmed E Amer wishes to thank the Egyptian Cultural Affairs and Missions Sector, as well as Port Said University and Saint-Petersburg Mining University for their financial support.

References

[1] M. M. Elsakka, D. B. Ingham, L Ma, M Pourkashanian. Comparison of the computational fluid dynamics predictions of vertical axis wind turbine performance against detailed pressure measurements. International Journal of Renewable Energy Research. 2021 Mar 30;11(1):276-93.

[2] M.A. Peretyatko, P.V. Yakovlev, V.A. Lebedev, A.S. Deev, The choice of fluid and thermal grid of the organic Rankine cycle in the conditions of its application at the oil refineries. Advances in Raw Material Industries for Sustainable Development Goals, London, 2020, p. 9 DOI: 10.1201/9781003164395-46

[3] M. M. Elsakka, D. B. Ingham, L Ma, M Pourkashanian. (2018). Effects of turbulence modelling on the predictions of the pressure distribution around the wing of a small scale vertical axis wind turbine. In Proceedings of the 6th European Conference on Computational Mechanics: Solids, Structures and Coupled Problems, ECCM 2018 and 7th European Conference on Computational Fluid Dynamics, ECFD (Vol. 2020, pp. 3921-3931).

[4] A. Refaat and M. H. Osman, “Current collector optimizer topology to improve maximum power from PV array under partial shading conditions,” IOP Conference Series: Materials Science and Engineering, vol. 643, no. 1, 2019.

[5] S. H Zanjani, H. Shahinzadeh, A. B. Oskui, W. Yaïci, M. Longo, and S. M. Zanjani (2022, June). Performance Assessment of Heat Pump and Solar Thermal Heating with Seasonal Storage Systems for Smart Microgrid Research Center Building at IAUN. In 2022 10th International Conference on Smart Grid (icSmartGrid) (pp. 345-350). IEEE.

[6] P. Angumba, A. Cárdenas, and D. Icaza (2022, June). Geothermal and Solar Energy Applied to Air Conditioning and Electricity Generation for Homes: Case study Baños in Cuenca-Ecuador. In 2022 10th International Conference on Smart Grid (icSmartGrid) (pp. 407-413). IEEE.

[7] S. Kyaligonza, and E. Cetkin (2021). Photovoltaic System Efficiency Enhancement with Thermal Management: Phase Changing Materials (PCM) with High Conductivity Inserts. Int. J. Smart grid, 5(4), 138-148.

[8] E. Mostafa, and N. K. Bahgaat (2017). A Comparison Between Using A Firefly Algorithm and A Modified PSO Technique for Stability Analysis of a PV System Connected to Grid. International Journal of Smart Grid-ijSmartGrid, 1(1), 1-8.

[9] K. Lentswe and A. Mawire (2022, September). Charging Energetic and Exergetic Evaluation of A Combined Solar Cooking and Thermal Energy

Storage System. In 2022 11th International Conference on Renewable Energy Research and Application (ICRERA) (pp. 71-76). IEEE.

[10] M. G. Osman, D. A. Ciupagenau, G. Lazaroiu, and I. Pisa (2022, September). Increasing Renewable Energy Participation in Sudan. In 2022 11th International Conference on Renewable Energy Research and Application (ICRERA) (pp. 169-173). IEEE.

[11] M. M. Elsakka, D. B. Ingham, L. Ma, M. Pourkashanian, G. H. Moustafa, and Y. Elhenawy (2022). Response surface optimisation of vertical axis wind turbine at low wind speeds. Energy Reports, 8, 10868-10880.

[12] M. H. Osman and A. Refaat (2019, November). Adaptive multi-variable step size P&O MPPT for high tracking-speed and accuracy. In IOP Conference Series: Materials Science and Engineering (Vol. 643, No. 1, p. 012050). IOP Publishing.

[13] F. Agyenim, N. Hewitt, P. Eames, and M. Smyth, "A review of materials, heat transfer and phase change problem formulation for latent heat thermal energy storage systems (LHTESS)," Renewable and Sustainable Energy Reviews, vol. 14, no. 2, pp. 615–628, 2010, doi: 10.1016/j.rser.2009.10.015.

[14] V. A. Lebedev and A. E. Amer, "Limitations of using phase change materials for thermal energy storage," in IOP Conference Series: Earth and Environmental Science, 2019, vol. 378, no. 1. doi: 10.1088/1755-1315/378/1/012044.

[15] A. E. A. Amer and V. Lebedev, "Thermal Energy Storage by Using Latent Heat Storage Materials," vol. 9, no. 5, pp. 1442–1447, 2018.

[16] K. S. Reddy, V. Mudgal, and T. K. Mallick, "Review of latent heat thermal energy storage for improved material stability and effective load management," Journal of Energy Storage, vol. 15, pp. 205–227, 2018, doi: 10.1016/j.est.2017.11.005.

[17] Y. Elhenawy, G. H. Moustafa, S. M. S. Abdel-Hamid, M. Bassyouni, and M. M. Elsakka, "Experimental investigation of two novel arrangements of air gap membrane distillation module with heat recovery," Energy Reports, vol. 8, pp. 8563–8573, Nov. 2022, doi: 10.1016/j.egyr.2022.06.068.

[18] M. Zakaria, A. M. Sharaky, A. S. Al-Sherbini, M. Bassyouni, M. Rezakazemi and Y. Elhenawy, "Water Desalination Using Solar Thermal Collectors Enhanced by Nanofluids," Chemical Engineering and Technology, vol. 45, no. 1, pp. 15–25, 2022.

[19] A. E. Amer, K. Rahmani, and V. A. Lebedev, "Using the Analytic Hierarchy Process (AHP) method for selection of phase change materials for solar energy storage applications," Journal of Physics: Conference Series, vol. 1614, p. 012022, Aug. 2020, doi: 10.1088/1742-6596/1614/1/012022.

[20] L. Socaciu, O. Giurgiu, D. Banyai, and M. Simion, "PCM selection using AHP method to maintain thermal comfort of the vehicle occupants," vol. 85, no. November 2015, pp. 489–497, 2016, doi: 10.1016/j.egypro.2015.12.232.

[21] M. H. Osman, M. A. E. Seify, M. K. Ahmed, N. V. Korovkin and A. Refaat, "Highly Efficient MPP Tracker Based on Adaptive Neuro-fuzzy Inference System for Stand-Alone Photovoltaic Generator System," International Journal of Renewable Energy Research, vol. 12, no. 1, pp. 209–217, 2022.

[22] M. J. Hosseini, M. Rahimi, and R. Bahrampoury, "Experimental and computational evolution of a shell and tube heat exchanger as a PCM thermal storage system," International Communications in Heat and Mass Transfer, vol. 50, pp. 128–136, 2014, doi: 10.1016/j.icheatmasstransfer.2013.11.008.

[23] M. Akgun, O. Aydin, and K. Kaygusuz, "Thermal energy storage behavior of a paraffin during melting and solidification," Energy Sources, Part A: Recovery, Utilization and Environmental Effects, vol. 29, no. 14, pp. 1315–1326, 2007, doi: 10.1080/00908310600710681.

[24] S. Seddegh, X. Wang, and A. D. Henderson, "A comparative study of thermal behaviour of a horizontal and vertical shell-and-tube energy storage using phase change materials," Applied Thermal Engineering, vol. 93, pp. 348–358, 2016, doi: 10.1016/j.applthermaleng.2015.09.107.

[25] A. E. Amer and V. A. Lebedev, Numerical investigations on latent heat storage unit using phase change material. InJournal of Physics: Conference Series 2020 Jun 1 (Vol. 1565, No. 1, p. 012099). IOP Publishing.

[26] G. ülseren Baran and A. Sari, "Phase change and heat transfer characteristics of a eutectic mixture of palmitic and stearic acids as PCM in a latent heat storage system," Energy Conversion and Management, vol. 44, no. 20, pp. 3227–3246, 2003, doi: 10.1016/S0196-8904(03)00104-3.

[27] Q. A. Jawad, A. M. Mahdy, A. H. Khuder, and M. T. Chaichan, (2020). Improve the performance of a solar air heater by adding aluminum chip, paraffin wax, and nano-SiC. Case Studies in Thermal Engineering, 19, 100622.

[28] E. F. Abbas, H. S. Sulaiman, and T. A Tahseen, (2021). Assessment of the Thermal Performance of Hybrid PVT Collector by Integrating it with a PCM Storage Unit. International Journal of Renewable Energy Research (IJRER), 11(3), 1043-1052.

[29] M. T. Chaichan, H. A. Kazem, A. H. Al-Waeli, and K. Sopian, (2021). Controlling the melting and solidification points temperature of PCMs on the performance and economic return of the water-cooled photovoltaic thermal system. Solar Energy, 224, 1344-1357.

[30] A. E. Amer, M. M. Elsakka, and V. A. Lebedev, "Thermal performance of an accumulator unit using phase change material with a fixed volume of fins," International Journal of Energy Research, vol. 45, no. 13, pp. 19089–19102, Oct. 2021, doi: 10.1002/er.7095.

[31] N. H. S. Tay, F. Bruno, and M. Belusko, "Comparison of pinned and finned tubes in a phase change thermal energy storage system using CFD," APPLIED ENERGY, vol. 104, pp. 79–86, 2013, doi: 10.1016/j.apenergy.2012.10.040.

[32] G. Ravi et al., "Numerical Heat Transfer, Part A : Applications Laminar Flow Forced Convection Heat Transfer Behavior of a Phase Change Material Fluid in Finned Tubes," vol. 7782, 2009, doi: 10.1080/10407780902864672.

[33] K. A. R. Ismail, C. L. F. Alves, and M. S. Modesto, "Numerical and experimental study on the solidification of PCM around a vertical axially finned isothermal cylinder," Applied Thermal Engineering, vol. 21, no. 1, pp. 53–77, 2001, doi: 10.1016/S1359-4311(00)00002-8.

[34] S. Deng, C. Nie, G. Wei, and W. Ye, "Energy & Buildings Improving the melting performance of a horizontal shell-tube latent-heat thermal energy storage unit using local enhanced finned tube," Energy & Buildings, vol. 183, pp. 161–173, 2019, doi: 10.1016/j.enbuild.2018.11.018.

[35] K. A. Aly, A. R. El-lathy, and M. A. Fouad, "Enhancement of solidification rate of latent heat thermal energy storage using corrugated fi ns," Journal of Energy Storage, vol. 24, no. January, p. 100785, 2019, doi: 10.1016/j.est.2019.100785.

[36] A. E. Amer and V. A. Lebedev, "Heat Storage with Phase Transition" doi: RU202391U1, Federal Service for Intellectual Property, Russia, 2020.

[37] A. D. Brent, V. R. Voller, and K. J. Reid, "Enthalpy-porosity technique for modeling convection-diffusion phase change: Application to the melting of a pure metal," Numerical Heat Transfer, vol. 13, no. 3, pp. 297–318, 1988, doi: 10.1080/10407788808913615.

[38] Patankar, S., and Flow, F. (1980). Hemisphere series on computational methods in mechanics and thermal science. Numerical Heat Transfer and Fluid Flow.

[39] M. J. Hosseini, A. A. Ranjbar, K. Sedighi, and M. Rahimi, "A combined experimental and computational study on the melting behavior of a medium temperature phase change storage material inside shell and tube heat exchanger," International Communications in Heat and Mass Transfer, vol. 39, no. 9, pp. 1416–1424, 2012, doi: 10.1016/j.icheatmasstransfer.2012.07.028.

[40] C. Guo and W. Zhang, "Numerical simulation and parametric study on new type of high temperature latent heat thermal energy storage system," Energy Conversion and Management, vol. 49, no. 5, pp. 919–927, May 2008.

[41] A. M. Abdulateef, S. Mat, K. Sopian, J. Abdulateef, and A. A. Gitan, "Experimental and computational study of melting phase-change material in a triplex tube heat exchanger with longitudinal/triangular fins," Solar Energy, vol. 155, pp. 142–153, 2017, doi: 10.1016/j.solener.2017.06.024.